European Journal of Nuclear Medicine and Molecular Imaging (2024) 51:907–918
https://doi.org/10.1007/s00259-023-06483-y

ORIGINAL ARTICLE

Diagnostic accuracy of fully hybrid [^{68}Ga]Ga-PSMA-11 PET/MRI and [^{68}Ga]Ga-RM2 PET/MRI in patients with biochemically recurrent prostate cancer: a prospective single-center phase II clinical trial

Samuele Ghezzo[1,2] · Paola Mapelli[1,2] · Ana Maria Samanes Gajate[2] · Anna Palmisano[1,3] · Vito Cucchiara[1,4] · Giorgio Brembilla[1,3] · Carolina Bezzi[1,2] · Nazareno Suardi[5] · Paola Scifo[2] · Alberto Briganti[1,4] · Francesco De Cobelli[1,3] · Arturo Chiti[1,2] · Antonio Esposito[1,3] · Maria Picchio[1,2]

Received: 15 June 2023 / Accepted: 16 October 2023 / Published online: 28 October 2023

Abstract

Purpose To compare the diagnostic accuracy and detection rates of PET/MRI with [^{68}Ga]Ga-PSMA-11 and [^{68}Ga]Ga-M2 in patients with biochemical recurrence of prostate cancer (PCa).

Methods Sixty patients were enrolled in this prospective single-center phase II clinical trial from June 2020 to October 2022. Forty-four/60 completed all study examinations and were available at follow-up (median: 22.8 months, range: 6–31.5 months). Two nuclear medicine physicians analyzed PET images and two radiologists interpreted MRI; images were then re-examined to produce an integrated PET/MRI report for both [^{68}Ga]Ga-PSMA-11 and [^{68}Ga]Ga-RM2 examinations. A composite reference standard including histological specimens, response to treatment, and conventional imaging gathered during follow-up was used to validate imaging findings. Detection rates, accuracy, sensitivity, specificity, positive, and negative predictive value were assessed. McNemar's test was used to compare sensitivity and specificity on a per-patient base and detection rate on a per-region base. Prostate bed, locoregional lymph nodes, non-skeletal distant metastases, and bone metastases were considered. *p*-value significance was defined below the 0.05 level after correction for multiple testing.

Results Patients' median age was 69.8 years (interquartile range (IQR): 61.8–75.1) and median PSA level at time of imaging was 0.53 ng/mL (IQR: 0.33–2.04). During follow-up, evidence of recurrence was observed in 31/44 patients. Combining MRI with [^{68}Ga]Ga-PSMA-11 PET and [^{68}Ga]Ga-RM2 PET resulted in sensitivity = 100% and 93.5% and specificity of 69.2% and 69.2%, respectively. When considering the individual imaging modalities, [^{68}Ga]Ga-RM2 PET showed lower sensitivity compared to [^{68}Ga]Ga-PSMA-11 PET and MRI (61.3% vs 83.9% and 87.1%, $p = 0.046$ and 0.043, respectively), while specificity was comparable among the imaging modalities (100% vs 84.6% and 69.2%, $p = 0.479$ and 0.134, respectively).

Conclusion This study brings further evidence on the utility of fully hybrid PET/MRI for disease characterization in patients with biochemically recurrent PCa. Imaging with [^{68}Ga]Ga-PSMA-11 PET showed high sensitivity, while the utility of [^{68}Ga]Ga-RM2 PET in absence of a simultaneous whole-body/multiparametric MRI remains to be determined.

Keywords PSMA · RM2 · PET/MRI · Prostate cancer · Biochemical recurrence · Diagnostic accuracy

Ghezzo S. and Mapelli P. equally contributed to the paper and therefore they are joint first authors.

Esposito A. and Picchio M. equally contributed to the paper and therefore they are joint last authors.

✉ Maria Picchio
picchio.maria@hsr.it

[1] Vita-Salute San Raffaele University, Via Olgettina 58, 20132 Milan, Italy

[2] Nuclear Medicine Department, IRCCS San Raffaele Scientific Institute, Via Olgettina 60, 20132 Milan, Italy

[3] Department of Radiology, IRCCS San Raffaele Scientific Institute, Via Olgettina 60, 20132 Milan, Italy

[4] Department of Urology and Division of Experimental Oncology, URI, Urological Research Institute, IRCCS San Raffaele Scientific Institute, Via Olgettina 60, 20132 Milan, Italy

[5] IRCCS Ospedale Policlinico San Martino, University of Genoa, Largo Benzi 10, 16132 Genoa, Italy

Introduction

Radical prostatectomy (RP) and external beam radiotherapy (EBRT) are the treatments of choice for primary localized prostate cancer (PCa). However, approximately 27–53% of patients still experience biochemical recurrence (BCR) [1]. Prostate specific antigen (PSA) is a reliable biomarker of disease recurrence after primary treatment; however, it cannot provide information on the exact sites of PCa recurrence. When BCR is diagnosed, an accurate identification of both location and extent of cancer recurrence is mandatory to initiate appropriate therapies aimed at improving survival [2]. Medical imaging is of the utmost importance in this context, as it drives the clinical management of patients with biochemically recurrent PCa.

Since its introduction in 2012, prostate-specific membrane antigen (PSMA) positron-emission tomography (PET) has showed higher sensitivity compared to conventional imaging modalities in characterizing primary PCa [3–6] and in localizing recurrent disease, even at low PSA levels [6–11]. PET with PSMA radioligands is currently recommended by the EAU-EANM-ESTRO-ESUR-ISUP-SIOG guidelines for the clinical management of PCa and it has become the gold standard imaging modality to restage patients with BCR of PCa [6].

New molecular probes demonstrated encouraging results in both the staging and restaging of PCa [12]. As gastrin releasing peptide receptors (GRPr) are G-protein coupled receptors overexpressed in 63–100% of human PCa tissue, GRPr analogues have been proposed as potential targets for molecular imaging in PCa [8, 13–15]. Among the available radioligands targeting GRPr, [^{68}Ga]Ga-RM2, an antagonistic PET tracer binding the human GRPr, showed promising results in detecting primary and recurrent disease [8, 14–18].

The clinical availability of integrated PET/MRI has proven its strength as a comprehensive imaging approach to investigate patients with biochemical recurrence of PCa. In fact, the combined simultaneous acquisition of PET and whole body/multiparametric MRI (mp-MRI) provides metabolic-receptor, structural, and functional imaging information regarding PCa status in a total body single session examination, with reduced radiation exposure and higher soft tissue contrast, required for imaging pelvic structures, compared to PET/CT [19–22].

While there is a great body of literature assessing the diagnostic accuracy of PSMA PET for the detection of recurrent PCa [7, 9, 23, 24] and an increasing number of studies comparing PSMA PET/CT and PSMA PET/MRI [19, 25–27], only few investigations compared PSMA and GRPr PET in the setting of biochemically recurrent PCa [8, 15, 16, 28]. Moreover, there are no currently available clinical trials performing a direct comparison between the diagnostic accuracy of fully hybrid PET/MRI with PSMA and GRPr radioligands in the same cohort of patients with biochemically recurrent PCa.

The primary aim of this study is to evaluate and compare the diagnostic accuracy of [^{68}Ga]Ga-PSMA-11 PET/MRI and [^{68}Ga]Ga-RM2 PET/MRI in patients with biochemically recurrent PCa. The secondary aim is to compare the patient and region-based detection rates of these imaging modalities. Additionally, the association between imaging findings and clinical/histopathological data is explored.

Materials and methods

Patients

In this prospective phase II clinical trial (EudraCT 2018–001036-21), 60 consecutive patients with biochemically recurrent PCa were enrolled from June 2020 to October 2022 at IRCCS San Raffaele. Inclusion criteria were (1) age greater than 18 years at the time of PET/MRI scan; (2) PCa patients treated with radical therapy (RP or radiotherapy (RT), with or without further adjuvant therapies); (3) biochemical recurrence of PCa, defined as two consecutive PSA measurements ≥ 0.2 ng/mL after RP or an increase by ≥ 2 ng/mL above the nadir PSA for patients previously treated with RT [29]. Exclusion criteria were (1) medical condition possibly interfering and significantly affecting study compliance and (2) contraindications to undergo MRI scan (i.e., severe claustrophobia).

All patients underwent [^{68}Ga]Ga-PSMA-11 PET/MRI; 50/60 also underwent [^{68}Ga]Ga-RM2 PET/MRI, in two different scan sessions, with at least 48 h interval (median time between scans: 2 days; range: 2–16 days).

As the primary aim of this study was to evaluate and compare the diagnostic accuracy of [^{68}Ga]Ga-PSMA-11 PET/MRI and [^{68}Ga]Ga-RM2 PET/MRI in detecting recurrent PCa, only patients who completed all study examinations were considered for the analyses.

Clinical data including PSA level at different time points, ISUP grade after RP (when available), age at time of PET/MR imaging acquisition, and time between radical treatment and biochemical recurrence were collected for all patients.

This study was approved by the Institutional Ethics Committee of IRCCS San Raffaele (26/INT/2018, approved on March 4th, 2020), and all patients gave written informed consent to participate to the study. Patients' characteristics are reported in Table 1.

[^{68}Ga]Ga-PSMA-11 PET/MRI acquisition protocol

Fasting was requested on the day of [^{68}Ga]Ga-PSMA-11 PET/MRI scan. Images were acquired on a Signa PET/

Table 1 Patients' characteristics, *IQR* interquartile range

	All patients ($N=60$)	All examinations and follow-up available ($N=44$)
Age, median (IQR), years	69.8 (61.8–75.1)	70.1 (62.8–74.6)
Initial therapy		
Prostatectomy only	36	26
Radiation therapy only	2	2
Prostatectomy and adjuvant radiation therapy	17	12
Prostatectomy and adjuvant radiation therapy + androgen deprivation therapy	5	4
ISUP grade		
1	6	3
2	13	9
3	15	11
4	12	9
5	14	12
Gleason score		
6 (3 + 3)	6	3
7 (3 + 4)	13	9
7 (4 + 3)	15	11
8 (4 + 4)	9	6
8 (5 + 3)	3	3
9 (4 + 5)	11	9
9 (5 + 4)	2	2
10 (5 + 5)	1	1
PSA, median (IQR), ng/mL	0.53 (0.33–2.04)	0.54 (0.38–2.18)
Time from initial therapy to imaging		
Median (IQR), months	52.8 (25.7–113.9)	50.25 (24.48–94.23)

MRI scanner (GE Healthcare, Waukesha, WI, USA) from the skull base to mid-thigh. The [^{68}Ga]Ga-PSMA-11 PET/MRI scan started 60 min (mean ± SD, 64 ± 17 min) after injection of 2 MBq per kilogram bodyweight (mean ± SD, 2.13 ± 0.36 MBq/kg) of [^{68}Ga]Ga-PSMA-11.

The [^{68}Ga]Ga-PSMA-11 PET/MR examination protocol included a high statistic scan of the pelvis (20 min), covering a single bed position, that was simultaneously acquired with a multiparametric MRI of the prostatic bed and pelvis including multiplanar T2 sequences, diffusion weighted imaging, and dynamic contrast-enhanced imaging. See Supplementary Table 1 for detailed information on the MR sequences.

Following the single bed acquisition, a total-body PET scan (5–6 FOVs, 4 min/FOV) was simultaneously acquired to a MRI total-body T1 Lava Flex sequence and a total-body DWI with $b=50$ and $b=1000$ s/mm^2. PET images were reconstructed using a Bayesian penalized likelihood reconstruction algorithm with a reconstructed FOV of 60 cm and image matrix of 192 × 192. The algorithm includes a Point Spread Function and Time of Flight information.

Attenuation Correction (AC) of PET data was performed using MR-Based AC technique based on the processing of the LAVA-Flex sequences acquired simultaneously with the PET data.

[^{68}Ga]Ga-RM2 PET/MRI acquisition protocol

As for [^{68}Ga]Ga-PSMA-11 PET/MRI, fasting was requested on the day of the examination and the same PET/MRI scanner was used. Image acquisition started 50 min (mean ± SD, 51 ± 12 min) after injection of 2 MBq per kilogram bodyweight (mean ± SD, 2.00 ± 0.31 MBq/kg) of [^{68}Ga]Ga-RM2. The [^{68}Ga]Ga-RM2 PET/MR examination protocol included a high statistic scan of the pelvis (20 min), covering a single bed position, that was simultaneously acquired with an axial T2 weighted sequence with large FOV (32 × 32 cm^2).

Following the single bed acquisition, a total-body PET scan (5–6 FOVs, 4 min/FOV) was acquired from the base of the skull to mid-thigh simultaneously with a MRI total-body Lava Flex sequence and total-body DWI with $b=50$ and $b=1500$ s/mm^2.

Based on the findings from the first [^{68}Ga]Ga-PSMA-11 examination, when lesions were found in the body, one or more specific MR sequences were acquired to better characterize the lesions. Reconstruction and attenuation correction

of PET images were performed using the same algorithms and parameters used for [^{68}Ga]Ga-PSMA-11 PET images.

PET/MR image evaluation

Images read-out was performed on the Advantage Workstation (AW, General Electric healthcare, Waukesha, WI, USA). A pool of two experienced nuclear medicine physicians (> 10 years of experience in prostate PET reading ad reporting) analyzed regional and total body [^{68}Ga]Ga-PSMA-11 PET and [^{68}Ga]-RM2 PET images. The whole-body distribution pattern of both [^{68}Ga]-PSMA-11 and [^{68}Ga]Ga-RM2 was qualitatively assessed, and the presence of increased uptake was considered positive for malignancy, except for areas of physiologically increased uptake [30, 31].

Qualitative examination of MR images was performed by a pool of three expert radiologists (> 10 years of experience in prostate MRI reading ad reporting). Local recurrence after RP was suspected in the presence of any soft tissue component within the surgical bed with abnormal signal on Dynamic Contrast-Enhanced (DCE) and Diffusion Weighted Imaging (DWI) sequences [32–34]. Similarly, local recurrence after RT was suspected in the presence of any focal abnormality within treated prostatic tissue characterized by abnormal signal on DCE and/or DWI [35–37]. For the definition of pathologic lymph nodes, a threshold of 10 mm in the short-axis for oval nodes and 8 mm for round nodes was used, also accounting for any signal abnormality on DWI sequences [38, 39]. Multi-sequence evaluation of all DWI images, DCE and morphologic sequences were undertaken to define the suspicion of distant metastases [40].

Nuclear medicine physicians and radiologists were not blinded to MRI and PET results, respectively.

Additionally, images were then re-evaluated by nuclear medicine physicians and radiologists in consensus to provide an integrated PET/MRI report for both [^{68}Ga]Ga-PSMA-11 and [^{68}Ga]Ga-RM2 PET/MRI examinations. Concordances and discrepancies between [^{68}Ga]Ga-PSMA-11 PET, [^{68}Ga]Ga-RM2 PET, MRI, [^{68}Ga]Ga-PSMA-11 PET/MRI, and [^{68}Ga]Ga-RM2 PET/MRI were defined with a qualitative comparison among the imaging modalities, on a per-patient and on a per-region base.

Regarding patient-based analysis, imaging modalities were defined concordant in case of positive or negative findings on both modalities.

For region-based analysis, prostate bed, locoregional lymph nodes, non-skeletal distant metastases, and bone metastases were considered as possible sites of recurrence and imaging modalities were defined concordant if (1) at least one pathological lesion was detected by both modalities or (2) if both scans resulted negative for the presence of pathological findings. In all remaining cases, the examinations were considered discordant.

Validation of imaging findings

Imaging findings were validated using a composite reference standard consisting in histopathologic confirmation whenever available ($n = 2$) or clinical and imaging follow-up (median follow-up: 22.8 months, IQR: 16.8–29.1 months) ($n = 42$).

Imaging findings were considered true positive when at least one of the following criteria was met: (1) histological confirmation performed on the surgical specimen of resected lesion; (2) progression on follow-up PSMA PET/CT or PET/MR studies (increase in number of lesions or increase in uptake, either on [^{68}Ga]Ga-PSMA-11 or [^{18}F]PSMA 1007) associated with an increase in PSA level; (3) confirmation on conventional imaging at follow-up; (4) disappearance or considerable reduction (i.e., number and intensity) of PSMA uptake on follow-up PET/CT or PET/MR scans after local or systemic treatment associated with a decrease in PSA level higher than 50%; and (5) decrease in PSA level greater than 50% after selective irradiation of the lesions.

Patients with negative imaging scans were considered true negative in the absence of evidence of disease during the follow-up period.

Patients without availability of histological validation or follow-up were excluded from the analyses. Forty-four patients were finally included in the study, as they completed all examinations and had availability of follow-up information. Figure 1 shows a flowchart of the patients' selection process.

Statistical analyses

Accuracy, sensitivity, specificity, positive, and negative predictive values (PPV and NPV) were calculated along with their 95% confidence intervals (CI) [41] on a per-patient base for all imaging modalities using the composite reference standard.

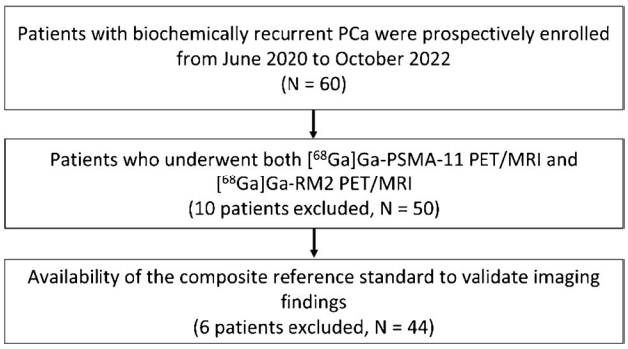

Fig. 1 Flowchart showing the patients' selection process

Detection rate was defined as the proportion of patients with positive imaging regardless of the reference standard, and it has been calculated for all imaging modalities over the full sample and stratifying the cohort based on PSA levels (PSA ≤ 0.5, PSA between 0.5 and 1, PSA between 1 and 2, and PSA ≥ 2). Concordance between imaging modalities was expressed by total agreement calculated between (1) [^{68}Ga]Ga-PSMA-11 PET and MRI; (2) [^{68}Ga]Ga-PSMA-11 PET and [^{68}Ga]Ga-RM2 PET; (3) [^{68}Ga]Ga-RM2 PET and MRI; and (4) [^{68}Ga]Ga-PSMA-11 PET/MRI and [^{68}Ga]Ga-RM2 PET/MRI by Cohen's Kappa value for the agreement beyond chance. Cohen's Kappa values were interpreted as follows: < 0.2 poor; 0.2–0.4 fair; 0.4–0.6 moderate; 0.6–0.8 substantial, and > 0.8 almost perfect agreement.

McNemar's test was used to compare sensitivity and specificity of all imaging modalities on a per-patient base and the detection rate of the investigated modalities on a per-region base.

Finally, univariable logistic regression was used to identify the predictors of positive imaging at (1) [^{68}Ga]Ga-PSMA-11 PET; (2) [^{68}Ga]Ga-RM2 PET; (3) MRI; (4) [^{68}Ga]Ga-PSMA-11 PET/MRI; and (5) [^{68}Ga]Ga-RM2 PET/MRI on a per-patient and per-region base. Analyses investigating the predictive role of PSA kinetics were based on data from 35/44 patients of whom more than one PSA measurement was available after radical treatment.

The higher probability of type I errors due to family-wise error rates was controlled by false discovery rate when appropriate. p-values < 0.05 were considered statistically significant. All statistical analyses were performed with R software v4.0.5 (R Foundation, Vienna, Austria) [42].

Results

Patient-based diagnostic accuracy

[^{68}Ga]Ga-PSMA-11 PET/MRI resulted in 35 patients with pathological findings, 31 of whom were confirmed as true positive by the composite reference standard. The 9 patients classified as negative by the integrated [^{68}Ga]Ga-PSMA-11 PET/MRI reports were all confirmed as true negative at follow-up. Therefore, the integrated examination of [^{68}Ga]Ga-PSMA-11 PET/MRI resulted in sensitivity = 100% (CI: 88.8–100%) and specificity = 69.2% (38.6–90.9%).

[^{68}Ga]Ga-RM2 PET/MRI detected recurrent PCa in 33 patients, 29 of whom were confirmed as true positive by the composite reference standard. Among the 11 patients classified as negative by the integrated examination of [^{68}Ga]Ga-RM2 PET and MR images, 9 were confirmed as true negative by the composite reference standard, hence resulting in sensitivity = 93.5% (CI: 78.6–99.2%) and specificity = 69.2% (38.6–90.9%) (Figs. 2, 3, and 4).

No significant differences were found comparing sensitivity and specificity of fully hybrid PET/MRI with either [^{68}Ga]Ga-PSMA-11 or [^{68}Ga]Ga-RM2 ($p = 0.479$ and 1, respectively).

However, when considering the imaging modalities individually, the composite reference standard confirmed 26/28 true positive and 11/16 true negative results at [^{68}Ga]Ga-PSMA-11 PET examination. Therefore, sensitivity and specificity for [^{68}Ga]Ga-PSMA-11 PET were 83.9% (CI: 66.3–94.5%) and 84.6% (CI: 54.6–98.1%), respectively. [^{68}Ga]Ga-RM2 PET findings were confirmed as true positive in 19/19 patients and true negative in 13/25 patients, yielding sensitivity and specificity of 61.3% (CI: 42.2–78.2%) and 100% (CI: 75.3–100%), respectively. Finally, 27/31 MRI positive findings were confirmed as true positive, with 9/13 being true negative according to the composite reference standard. Consequently, sensitivity and specificity for MRI were 87.1% (CI: 70.2–96.4%) and 69.2% (CI: 38.6–90.9%).

[^{68}Ga]Ga-RM2 PET showed lower sensitivity compared to [^{68}Ga]Ga-PSMA-11 PET and MRI ($p = 0.046$ and 0.043, respectively), while specificity was comparable among the imaging modalities ($p = 0.479$ and 0.134; respectively; Fig. 2a, b). Table 2 shows accuracy, sensitivity, specificity, positive predicted value, negative predicted value, and the corresponding 95% CI for all imaging modalities.

Patient-based detection rate

Thirty-five out of 44 patients (79.55%) were positive on integrated [^{68}Ga]Ga-PSMA-11 PET/MRI and 33/44 patients (75%) were positive on integrated [^{68}Ga]Ga-RM2 PET/MRI. All patients with evidence of recurrent PCa at [^{68}Ga]Ga-RM2 PET/MRI were also positive at [^{68}Ga]Ga-PSMA-11 PET/MRI examination, while the latter was positive in 2 additional cases, thus resulting in an almost perfect agreement between modalities (Cohen's Kappa = 0.87; CI: 0.7–1). [^{68}Ga]Ga-PSMA-11 PET was positive in 28/44 patients (63.64%), while [^{68}Ga]Ga-RM2 was positive in 19/44 patients (43.18%). PET examinations were concordant in 33/44 patients (18 patients positive at both scans, 15 negative) and discordant in 11/44 patients, 10 of which positive at [^{68}Ga]Ga-PSMA-11 PET. Therefore, there was a moderate agreement between the 2 modalities (Cohen's Kappa = 0.52; CI: 0.29–0.75). MRI was positive in 31/44 patients (70.45%). MRI and [^{68}Ga]Ga-PSMA-11 PET were concordant in 33/44 patients (24 patients with, and 9 without evidence of PCa recurrence in both modalities). Among the 11/44 discordant cases, 4 were positive at

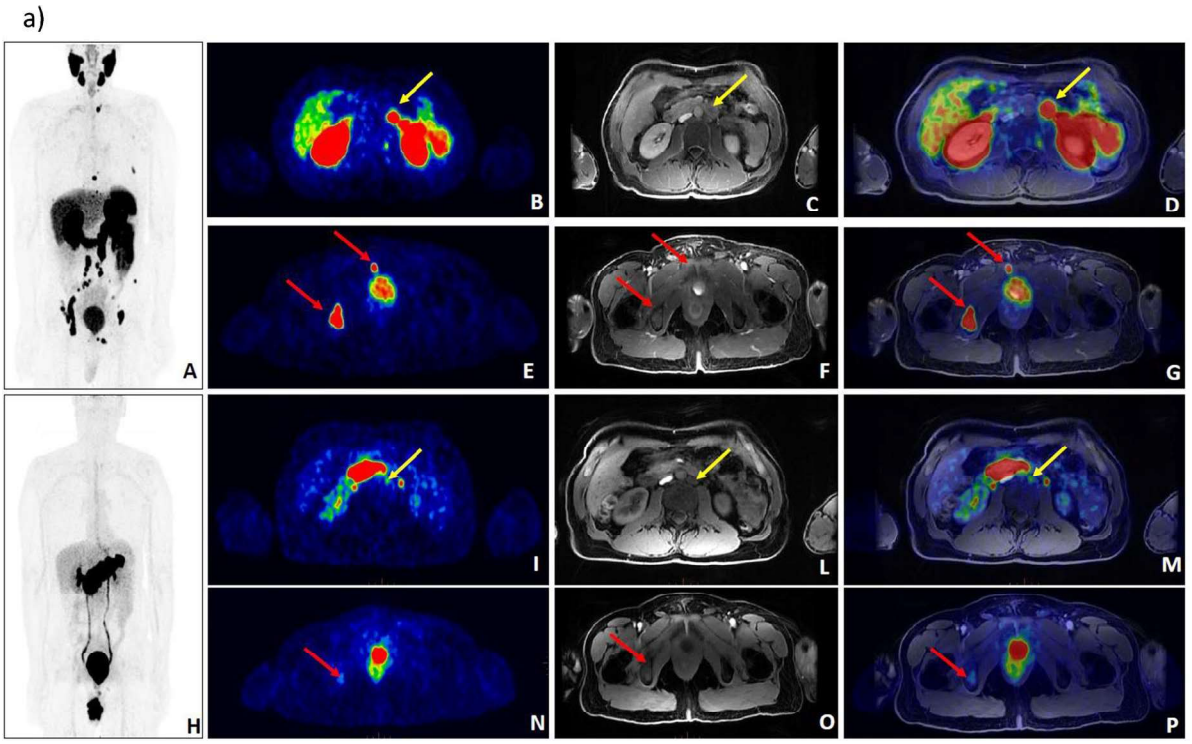
a)
A
B
C
D
E
F
G
H
I
L
M
N
O
P

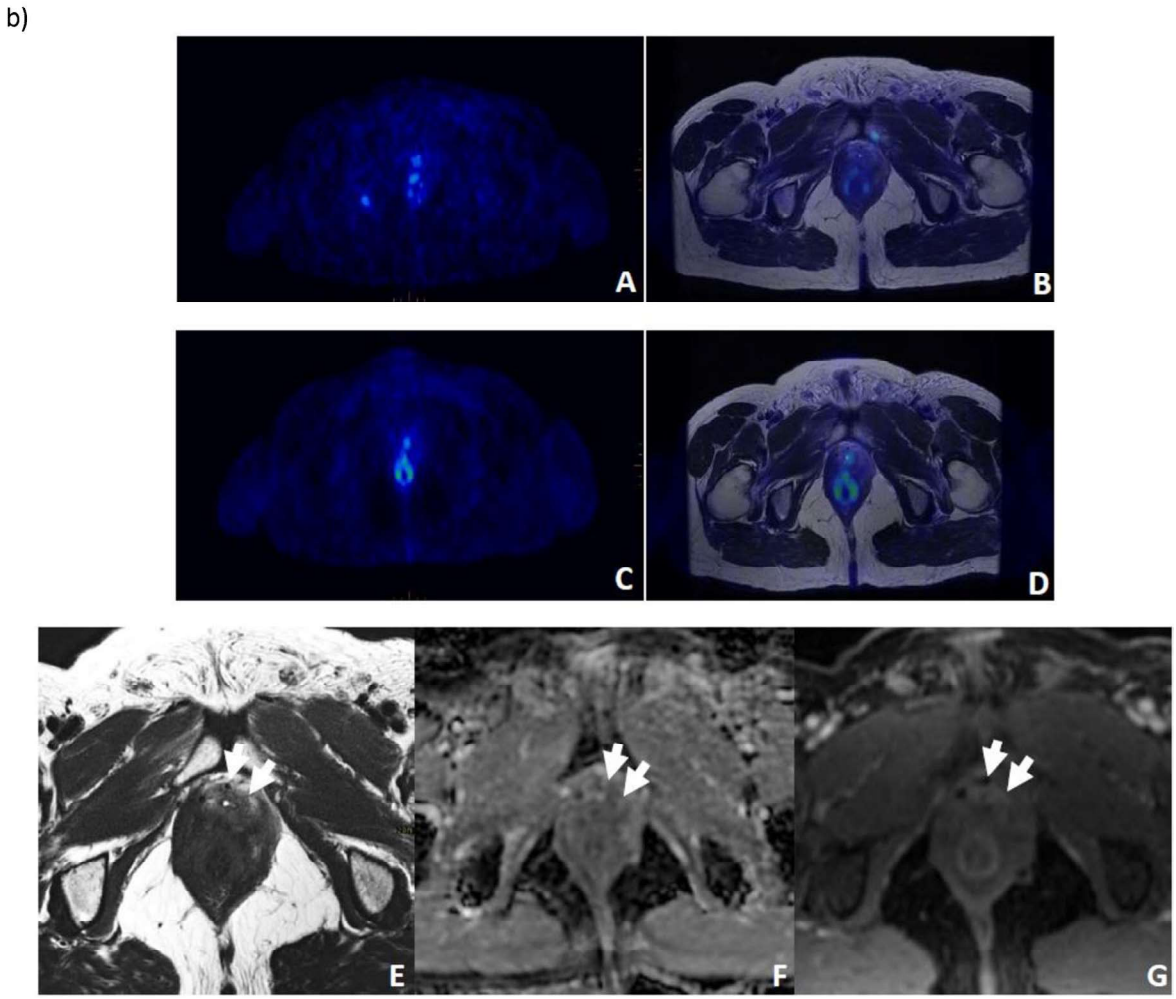
b)
A
B
C
D
E
F
G

◂**Fig. 2** **a** A 52-year-old patient previously treated with radical prostatectomy for PCa (Gleason 5 + 5 pT4N1M1aR1) underwent [^{68}Ga]Ga-PSMA-11 and [^{68}Ga]Ga-RM2 PET/MRI scan for biochemical recurrence (PSA = 14.4 ng/ml). [^{68}Ga]Ga-PSMA-11 PET showed multiple intense pathological bone and lymph nodal uptakes (**A** major intensity projection—MIP). In **B**, **C**, and **D** (transaxial PET, MR, and PET/MR images, respectively) pathological uptake is present in correspondence of a left paraortic lymphadenopathy (yellow arrows). In **E**, **F**, and **G** pathological bone uptake in the pelvis is depicted on PET images (red arrows). [^{68}Ga]Ga-RM2 PET showed a lower number of pathological bone and lymphnodal uptake compared to [^{68}Ga]Ga-PSMA-11 PET (**H** major intensity projection—MIP); in particular, **I**, **L**, and **M** show moderate radiotracer uptake in correspondence of the left paraortic lymph node (yellow arrows). In **N**, **O**, and **P** only a moderate pathological [^{68}Ga]Ga-RM2 bone uptake is depicted in correspondence of the right ischial tuberosity (red arrows). **b** The same patient as per **a** had no local recurrence in the prostatic bed according to transaxial [^{68}Ga]Ga-PSMA-11 PET and PET/MR images (**A** and **B**, respectively) and transaxial [^{68}Ga]Ga-RM2 PET and PET/MR images (**C** and **D**, respectively). MR images simultaneously acquired with PET images showed an area of increased wall thickness of the anterior border of the vescico-urethral anastomosis (arrows in **E**; T2 sequence), associated to slight restriction of diffusion (arrows in **F**; ADC sequence), and increased enhancement (arrows in **G**; T1 dynamic study). Multiple bone and nodal lesion were also detected on MR images in correspondence of the spine and of lymph node in the abdominal regions (images not shown)

[^{68}Ga]Ga-PSMA-11 PET and 7 at MRI. Hence, there was a moderate agreement between the imaging modalities (Cohen's Kappa = 0.44; CI: 0.16–0.82). [^{68}Ga]Ga-RM2 PET and MRI were concordant in 28/44 patients (17 patients positive at both exams, 11 negative) and discordant in the remaining 16/44, only two of which were positive at [^{68}Ga]Ga-RM2 PET. This resulted in a fair agreement between the 2 modalities (Cohen's Kappa = 0.31; CI: 0.078–0.54). See Supplementary Fig. 1 for the detection rate of [^{68}Ga]Ga-PSMA-11 PET/MRI and [^{68}Ga]Ga-RM2 PET/MRI stratified on PSA levels.

Region-based detection rate

The integration of [^{68}Ga]Ga-PSMA-11 PET and MRI findings, led to the identification of locally recurrent PCa in 17 patients, involvement of locoregional lymph nodes in 15 patients, non-skeletal distant metastases in 10 patients, and bone metastases in 14 patients. The integrated assessment of both [^{68}Ga]Ga-RM2 PET and MRI findings resulted in 15 patients positive for local recurrence of PCa, 13 patients with evidence of locoregional lymph nodes involvement, 6 with non-skeletal distant metastases and 11 patients positive for bone metastases. The detection rates of [^{68}Ga]Ga-PSMA-11 PET/MRI and [^{68}Ga]Ga-RM2 PET/MRI were comparable in all the investigated sites of recurrence ($p > 0.05$).

Considering the imaging modalities individually, [^{68}Ga]Ga-PSMA-11 PET identified locally recurrent PCa in 10 patients (detection rate improved by the integration with MRI, from 10 to 17 positive patients, although statistical significance was not confirmed after correction for multiple testing). [^{68}Ga]Ga-RM2 PET, on the other hand, detected locally recurrent PCa in 5 patients and locoregional lymph nodes in 6 patients (detection rates significantly improved by the integration with MRI $p = 0.016$ and $p = 0.046$, respectively). MRI detected locally recurrent PCa in 15 patients, 10 of whom were missed by [^{68}Ga]Ga-RM2 PET ($p = 0.012$). Conversely, MRI and [^{68}Ga]Ga-PSMA-11 PET showed comparable detection rates for local recurrence of PCa ($p = 0.182$). No other significant differences across the three investigated imaging modalities were found for all the other investigated sites of recurrence ($p > 0.05$). See Fig. 5 for the region-based detection rate of imaging. Detailed information regarding per-region base concordances across the investigated imaging modalities and the relative statistics can be found in supplementary Table 2.

Association between clinical data and imaging findings

Univariable logistic regression analyses assessing the association between clinical data and imaging findings are shown in Supplementary Tables 3–7. ISUP grade predicted the positivity at MRI and [^{68}Ga]Ga-RM2 PET/MRI (OR = 1.83 and 2.23; $p = 0.039$ and 0.016, respectively). However, these associations were not confirmed after correction for multiple testing. No other significant associations were found between the clinical/histopathological and imaging data.

Discussion

The present study represents the first phase II clinical trial comparing the diagnostic accuracy of fully hybrid PET/MRI with [^{68}Ga]Ga-PSMA-11 and [^{68}Ga]Ga-RM2 in localizing recurrent PCa. So far, only few studies have investigated the role of [^{68}Ga]Ga-RM2 PET in patients with BCR of PCa [8, 14, 15]. Among these, images were sporadically acquired using fully hybrid PET/MRI scanners, but only PET imaging was considered for analysis [8, 15]. Conversely, in the present work, both the diagnostic accuracy of [^{68}Ga]Ga-RM2 PET and [^{68}Ga]Ga-PSMA-11 PET and the additional value provided by the simultaneous whole-body/multiparametric MRI examination were investigated. Moreover, the detection rates of the investigated imaging modalities were compared on a per-patient and per-region base, and the associations between clinical/histopathological data and imaging findings were assessed.

The combination of [^{68}Ga]Ga-PSMA-11 PET and MRI in an integrated report led to the correct identification of all patients with evidence of PCa recurrence at follow-up, resulting in a sensitivity of 100%, thus bringing further evidence on the utility of fully hybrid PET/MRI as a one-stop

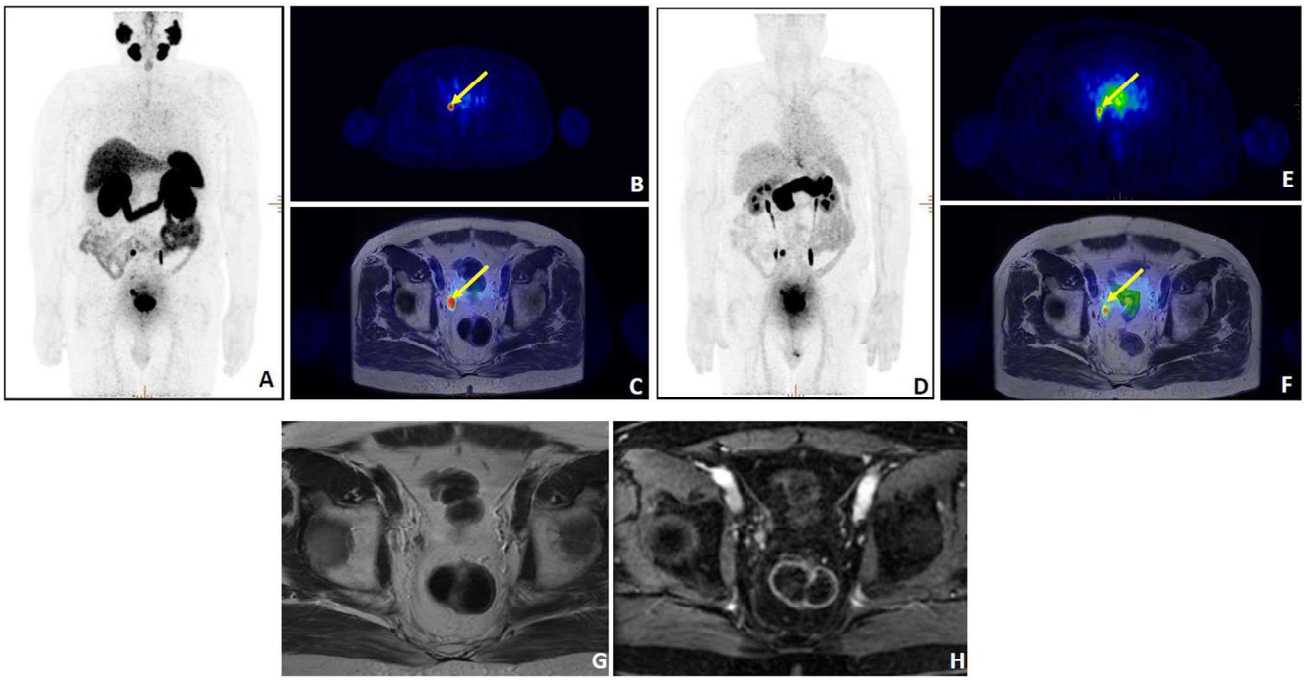

Fig. 3 A 74-year-old patient previously treated with radical prostatectomy for PCa (Gleason 9, pT3b pN0.) and adjuvant radiotherapy underwent [^{68}Ga]Ga-PSMA-11 and [^{68}Ga]Ga-RM2 PET/MRI scan for biochemical recurrence (PSA = 0.74 ng/ml). [^{68}Ga]Ga-PSMA-11 (**A** MIP; **B** transaxial PET; **C** transaxial PET/MRI) and [^{68}Ga]Ga-RM2 PET (**D** MIP; **E** transaxial PET; **F** transaxial PET/MRI, respectively) images showed increased radiotracer uptake in correspondence of the right obturator region (yellow arrows). High resolution T2 images (**G**) and post-contrast T1fatSat images (**H**) showed in the right obturatory region the presence of a lymph node increased in size, with round shape and inhomogeneous signal intensity and enhancement, suspected for nodal metastasis

shop for the characterization of biochemically recurrent PCa [20, 21]. Similarly, combining [^{68}Ga]Ga-RM2 PET and MRI resulted in high sensitivity (93.5%). Conversely, when assessing the diagnostic performance of individual imaging modalities [^{68}Ga]Ga-RM2 PET showed a limited sensitivity compared to both [^{68}Ga]Ga-PSMA-11 PET and MRI in identifying the sites of PCa recurrence, with comparable specificity.

The combination of PET and MRI increased the detection rate of both [^{68}Ga]Ga-PSMA-11 (from 63.64 to 79.55%) and [^{68}Ga]Ga-RM2 PET (from 43.18 to 75%). While these results are in line with a recent meta-analysis reporting a detection rate between 54.5 and 97% for PSMA PET/MRI in the identification of recurrent PCa [20], all patients with positive [^{68}Ga]Ga-RM2 PET/MRI had also a positive [^{68}Ga]Ga-PSMA-11 PET/MR, raising questions on the effective clinical utility of [^{68}Ga]Ga-RM2 PET.

The agreement between modalities showed a clear benefit deriving from the integration of MRI and PET images, as indicated by the increase in Cohen's Kappa value going from a moderate agreement between the 2 PET examinations to an almost perfect agreement between [^{68}Ga]Ga-PSMA-11 PET/MRI and [^{68}Ga]Ga-RM2 PET/MRI.

Our results showed similar detection rates for [^{68}Ga]Ga-PSMA-11 PET and MRI on a patient level, with [^{68}Ga]Ga-RM2 PET identifying recurrent disease in fewer cases. These findings are consistent with the preliminary data reported by our group [8], but showed dissimilarity with the data published by Baratto and colleagues [15], where similar detection rates for [^{68}Ga]Ga-PSMA-11 and [^{68}Ga]Ga-RM2 PET were found at patient level.

[^{68}Ga]Ga-PSMA-11 PET performance for the detection of local recurrence was improved when combined with MRI, while it was minimally affected for the detection of lymph node recurrence, due to the well-known high sensitivity of [^{68}Ga]Ga-PSMA-11 PET [6]. [^{68}Ga]Ga-RM2 PET identified a lower number of local and nodal recurrences compared to MRI and [^{68}Ga]Ga-PSMA-11 PET; and its detection rate was significantly improved when combining MRI and PET findings. Considering that the determination of metastatic lymph nodes with morphological imaging is largely determined by size, the possibility to have an integrated morpho-functional imaging modality, such as PET/MRI, combining functional information provided by the PET component, surely represent an asset in term of improved assessment of biochemical recurrent disease. The combination of PET and MRI did not impact the performance of PET examinations in the other considered regions of recurrence.

In our cohort, low serum levels of PSA were observed, possibly explaining also the lack of correlation between PSA

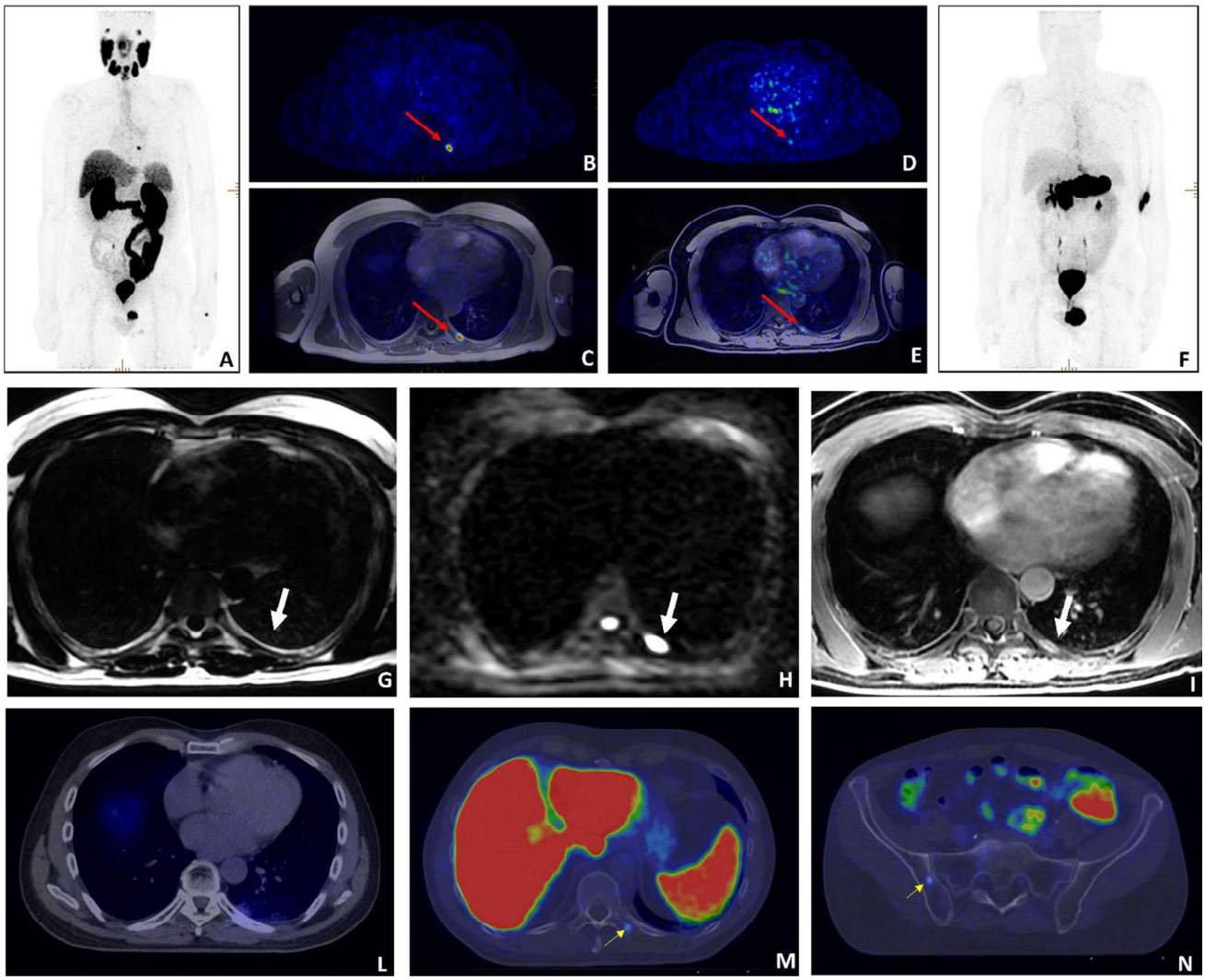

Fig. 4 A 63-year-old patient previously treated with radical prostatectomy for PCa (Gleason 9) underwent [^{68}Ga]Ga-PSMA-11 and [^{68}Ga]Ga-RM2 PET/MRI scan for biochemical recurrence (PSA = 0.34 ng/ml). [^{68}Ga]Ga-PSMA-11 PET images (**A** MIP; **B** transaxial PET; **C** transaxial PET/MRI) showed high and focal radiotracer uptake in correspondence of the posterolateral tract of the left IX rib (red arrows); [^{68}Ga]Ga-RM2 PET images (**D** transaxial PET; **E** transaxial PET/MRI, **F** MIP, respectively) showed moderate focal uptake in correspondence of the same bone finding. On LAVA flex image a hypointense lesion of 1.5 cm involving the posterolateral tract of the IX left rib was visible (arrow in **G**). This lesion was characterized by hyperintensity on DWIBS b 1000 image (arrow in **H**), as for restricted diffusion and increased contrast enhancement (arrow in **I**), referable to bone metastasis. The patient subsequently underwent to radiation treatment of the rib with a reduction of the PSA serum level and a negative [^{18}F]-PSMA 1007 PET scan performed during follow-up (**L** transaxial PET/CT). A subsequent further increase of PSA level (3.35 ng/mL) was then observed; a further [^{18}F]-PSMA 1007 PET scan showed pathological uptake in correspondence of the left transverse process of the XI thoracic vertebra (**M** transaxial PET/CT; yellow arrow) and of the right iliac wing (**N** transaxial PET/CT; yellow arrow) and hormone therapy was then initiated

Table 2 Patient-based diagnostic accuracy

	Accuracy (CI)	Sensitivity (CI)	Specificity (CI)	PPV (CI)	NPV (CI)
[^{68}Ga]Ga-PSMA-11 PET/MRI	0.909 (0.783–0.975)	0.818 (0.673–0.918)	0.692 (0.386–0.909)	0.886 (0.733–0.968)	1 (0.664–1)
[^{68}Ga]Ga-RM2 PET/MRI	0.864 (0.726–0.948)	0.935 (0.786–0.992)	0.692 (0.386–0.909)	0.879 (0.718–0.966)	0.818 (0.482–0.977)
[^{68}Ga]Ga-PSMA-11 PET	0.841 (0.699–0.934)	0.818 (0.482–0.977)	0.846 (0.546–0.981)	0.929 (0.765–0.981)	0.688 (0.413–0.890)
[^{68}Ga]Ga-RM2 PET	0.727 (0.572–0.850)	0.613 (0.422–0.782)	1 (0.753–1)	1 (0.824–1)	0.520 (0.313–0.722)
MRI	0.818 (0.673–0.918)	0.871 (0.702–0.964)	0.692 (0.386–0.909)	0.871 (0.702–0.964)	0.692 (0.386–0.909)

Patient-based diagnostic accuracy of [^{68}Ga]Ga-PSMA-11 PET/MRI, [^{68}Ga]Ga-RM2 PET/MRI, [^{68}Ga]Ga-PSMA-11 PET, [^{68}Ga]Ga-RM2 PET, and MRI. 95% confidence intervals in brackets

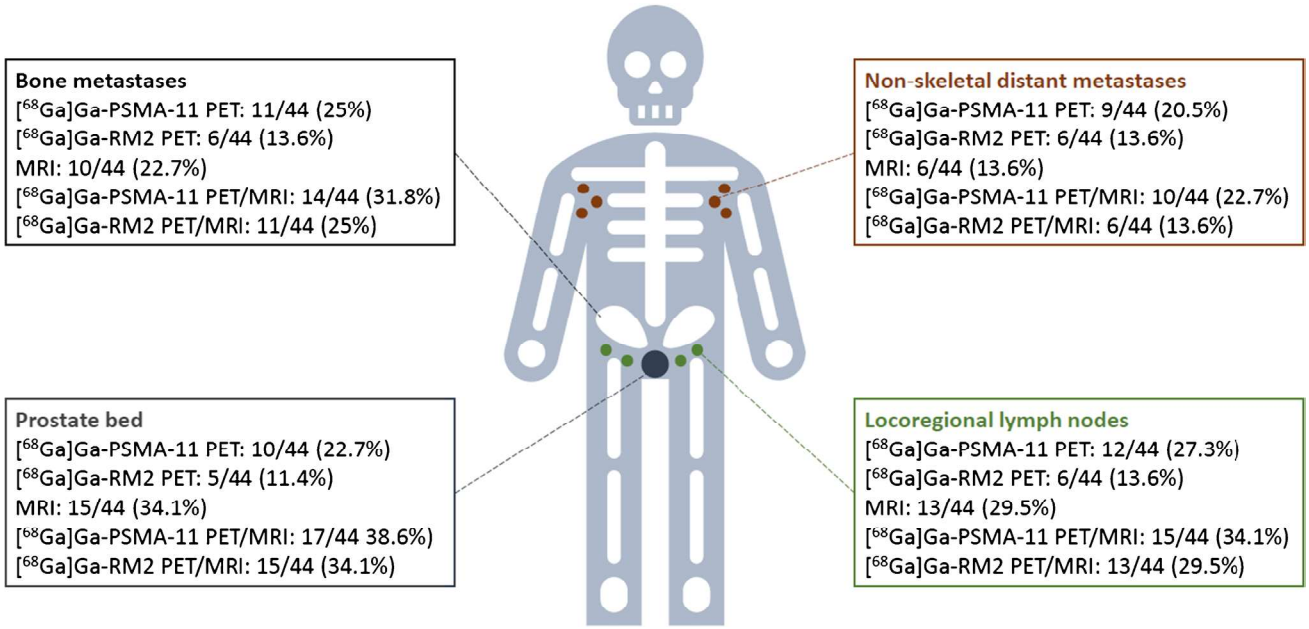

Fig. 5 Region-based detection rate of [^{68}Ga]Ga-PSMA-11 PET, [^{68}Ga]Ga-RM2 PET, MRI, [^{68}Ga]Ga-PSMA-11 PET/MRI, and [^{68}Ga]Ga-RM2 PET/MRI

and imaging findings observed in other studies [9]. Usually, patients with lower serum PSA levels have better oncologic outcomes compared to advanced stages, in view of the lower metastatic burden. Therefore, the possibility to detect PCa recurrence at very low PSA level, with a non-invasive imaging technique, may certainly improve patients' outcome.

A strength of the present study compared to previous works [15, 43, 44] is the composite reference standard used to validate imaging findings, providing clear indications on their diagnostic accuracy. Furthermore, all patients were prospectively enrolled and underwent both fully hybrid [^{68}Ga]Ga-PSMA-11 PET/MRI and [^{68}Ga]Ga-RM2 PET/MRI, allowing to investigate the utility of PET with a simultaneous whole-body/multiparametric MRI examination.

A limitation of this study is that it is a monocentric clinical trial with a small sample size. This, paired with the limited number of patients without evidence of PCa during follow-up, especially hampered the analysis comparing the specificity of the investigated imaging modalities. However, to date, this is the largest study comparing [^{68}Ga]Ga-PSMA-11 PET/MRI and [^{68}Ga]Ga-RM2 PET/MRI in the same cohort of patients with biochemically recurrent PCa, and the only one evaluating the additional value of a simultaneous whole-body/multiparametric MRI in this setting.

Another constraint is the lack of post-hoc correlation of imaging findings with histopathological results for all patients. However, this is consistent with the disease management of these patients, as a number of findings detected on PET/MRI are located in sites that are not usually considered for biopsy (i.e., bone) and/or are directly treated without any further confirmation (i.e., radiotherapy on positive lymph nodes, ADT).

Moreover, considering that some patients had a high number of metastases, the validation of imaging findings was not feasible at the level of all single lesions. Therefore, diagnostic accuracy was only feasible at patient-level, while the detection rate of all investigated imaging modalities was reported both at the patient- and region-level, providing detailed information on their performance.

Conclusions

This prospective monocentric phase II clinical trial showed the high diagnostic accuracy of fully hybrid PET/MRI with [^{68}Ga]Ga-PSMA-11 for the localization of biochemically recurrent PCa. We observed high sensitivity and specificity for [^{68}Ga]Ga-PSMA-11 PET, while the utility of [^{68}Ga]Ga-RM2 PET in these patients remains to be determined.

Supplementary Information The online version contains supplementary material available at https://doi.org/10.1007/s00259-023-06483-y.

Funding This research was funded by the Italian Ministry of Health (Project GR-2016–02363991-EUDRACT number: 2018–001036-21). Fully hybrid 3 Tesla PET/MRI system (SIGNA PET/MRI; General Electric Healthcare, Waukesha, WI, USA) was purchased with funding from Italian Ministry of Health.

Data Availability The datasets generated during the current study are available from the corresponding author on reasonable request.

Declarations

Ethical approval This study was approved by the Institutional Ethics Committee of IRCCS San Raffaele Scientific Institute. All procedures performed in studies involving human participants were in accordance with the ethical standards of the Institutional and national research committee and with the 1964 Helsinki Declaration and its later amendments or comparable ethical standards.

Consent to participate All patients gave their informed consent to participate to the study.

Conflict of interest The authors declare no competing interests.

References

1. Cornford P, van den Bergh RCN, Briers E, et al. EAU-EANM-ESTRO-ESUR-SIOG guidelines on prostate cancer. Part II—2020 update: treatment of relapsing and metastatic prostate cancer. Eur Urol. 2021;79:263–82.
2. Ploussard G, Almeras C, Briganti A, et al. Management of node only recurrence after primary local treatment for prostate cancer: a systematic review of the literature. J Urol. 2015;194:983–8.
3. Afshar-Oromieh A, Haberkorn U, Eder M, Eisenhut M, Zechmann C. [68Ga]Gallium-labelled PSMA ligand as superior PET tracer for the diagnosis of prostate cancer: comparison with 18F-FECH. Eur J Nucl Med Mol Imaging. 2012;39:1085–6.
4. Farolfi A, Calderoni L, Mattana F, et al. Current and emerging clinical applications of PSMA PET diagnostic imaging for prostate cancer. J Nucl Med. 2021;62:596–604.
5. Hofman MS, Lawrentschuk N, Francis RJ, et al. Prostate-specific membrane antigen PET-CT in patients with high-risk prostate cancer before curative-intent surgery or radiotherapy (proPSMA): a prospective, randomised, multicentre study. Lancet. 2020;395:1208–16.
6. Mottet N, Cornford P, Van den Bergh RCN, Briers E, Eberli D, De Meerleer G, De Santis M, Gillessen S, Grummet J, et al. EAU - EANM - ESTRO - ESUR - ISUP - SIOG guidelines on prostate cancer 2023. https://d56bochluxqnz.cloudfront.net/documents/full-guideline/EAU-Guidelines-on-Urological-infections-2023.pdf.
7. Luiting HB, van Leeuwen PJ, Busstra MB, et al. Use of gallium-68 prostate-specific membrane antigen positron-emission tomography for detecting lymph node metastases in primary and recurrent prostate cancer and location of recurrence after radical prostatectomy: an overview of the current literature. BJU Int. 2020;125:206–14.
8. Mapelli P, Ghezzo S, Samanes Gajate AM, et al. 68Ga-PSMA and 68Ga-DOTA-RM2 PET/MRI in recurrent prostate cancer: diagnostic performance and association with clinical and histopathological data. Cancers (Basel). 2022;14:334.
9. Fendler WP, Calais J, Eiber M, et al. Assessment of 68 Ga-PSMA-11 PET accuracy in localizing recurrent prostate cancer. JAMA Oncol. 2019;5:856.
10. Han S, Woo S, Kim YJ, Suh CH. Impact of 68 Ga-PSMA PET on the management of patients with prostate cancer: a systematic review and meta-analysis. Eur Urol. 2018;74:179–90.
11. Morris MJ, Rowe SP, Gorin MA, et al. Diagnostic performance of 18F-DCFPyL-PET/CT in men with biochemically recurrent prostate cancer: results from the CONDOR phase III, multicenter study. Clin Cancer Res. 2021;27:3674–82.
12. Mena E, Lindenberg LM, Choyke PL. New targets for PET molecular imaging of prostate cancer. Semin Nucl Med. 2019;49:326–36.
13. Körner M, Waser B, Rehmann R, Reubi JC. Early over-expression of GRP receptors in prostatic carcinogenesis. Prostate. 2014;74:217–24.
14. Wieser G, Popp I, Christian Rischke H, et al. Diagnosis of recurrent prostate cancer with PET/CT imaging using the gastrin-releasing peptide receptor antagonist 68Ga-RM2: preliminary results in patients with negative or inconclusive [18F] Fluoroethylcholine-PET/CT. Eur J Nucl Med Mol Imaging. 2017;44:1463–72.
15. Baratto L, Song H, Duan H, et al. PSMA- and GRPR-targeted PET: results from 50 patients with biochemically recurrent prostate cancer. J Nucl Med. 2021;62:1545–9.
16. Mapelli P, Ghezzo S, Samanes Gajate AM, et al. Preliminary results of an ongoing prospective clinical trial on the use of 68Ga-PSMA and 68Ga-DOTA-RM2 PET/MRI in staging of high-risk prostate cancer patients. Diagnostics. 2021;11:2068.
17. Iagaru A. Will GRPR compete with PSMA as a target in prostate cancer? J Nucl Med. 2017;58:1883–4.
18. Duan H, Iagaru A. PET imaging using gallium-68 (68Ga) RM2. PET Clin. 2022;17:621–9.
19. Liu FY, Sheng TW, Tseng JR, Yu KJ, Tsui KH, Pang ST, Wang LJ, Lin G. Prostate-specific membrane antigen (PSMA) fusion imaging in prostate cancer: PET-CT vs PET-MRI. Br J Radiol. 2022;95(1131):20210728. https://doi.org/10.1259/bjr.20210728.
20. Evangelista L, Zattoni F, Cassarino G, et al. PET/MRI in prostate cancer: a systematic review and meta-analysis. Eur J Nucl Med Mol Imaging. 2021;48:859–73.
21. Freitag MT, Radtke JP, Afshar-Oromieh A, et al. Local recurrence of prostate cancer after radical prostatectomy is at risk to be missed in 68Ga-PSMA-11-PET of PET/CT and PET/MRI: comparison with mpMRI integrated in simultaneous PET/MRI. Eur J Nucl Med Mol Imaging. 2017;44:776–87.
22. Afshar-Oromieh A, Haberkorn U, Schlemmer HP, et al. Comparison of PET/CT and PET/MRI hybrid systems using a 68Ga-labelled PSMA ligand for the diagnosis of recurrent prostate cancer: initial experience. Eur J Nucl Med Mol Imaging. 2014;41:887–97.
23. Hoffmann MA, Wieler HJ, Baues C, et al. The impact of 68Ga-PSMA PET/CT and PET/MRI on the management of prostate cancer. Urology. 2019;130:1–12.
24. Sonni I, Eiber M, Fendler WP, et al. Impact of 68 Ga-PSMA-11 PET/CT on staging and management of prostate cancer patients in various clinical settings: a prospective single-center study. J Nucl Med. 2020;61:1153–60.
25. Huo H, Shen S, He D, Liu B, Yang F. Head-to-head comparison of 68Ga-PSMA-11 PET/CT and 68Ga-PSMA-11 PET/MRI in the detection of biochemical recurrence of prostate cancer: summary of head-to-head comparison studies. Prostate Cancer Prostatic Dis. 2023;26(1):16–24. https://doi.org/10.1038/s41391-022-00581-y.
26. Glemser PA, Rotkopf LT, Ziener CH, et al. Hybrid imaging with [68Ga]PSMA-11 PET-CT and PET-MRI in biochemically recurrent prostate cancer. Cancer Imaging. 2022;22:53.
27. Jentjens S, Mai C, Ahmadi Bidakhvidi N, et al. Prospective comparison of simultaneous [68Ga]Ga-PSMA-11 PET/MR versus PET/CT in patients with biochemically recurrent prostate cancer. Eur Radiol. 2022;32:901–11.
28. Fassbender TF, Schiller F, Zamboglou C, et al. Voxel-based comparison of [68Ga]Ga-RM2-PET/CT and [68Ga]Ga-PSMA-11-PET/CT with histopathology for diagnosis of primary prostate cancer. EJNMMI Res. 2020;10:62.
29. Roach M, Hanks G, Thames H, et al. Defining biochemical failure following radiotherapy with or without hormonal therapy in men with clinically localized prostate cancer: recommendations of

the RTOG-ASTRO Phoenix Consensus Conference. Int J Radiat Oncol. 2006;65:965–74.
30. Demirci E, Sahin OE, Ocak M, et al. Normal distribution pattern and physiological variants of 68Ga-PSMA-11 PET/CT imaging. Nucl Med Commun. 2016;37:1169–79.
31. Baratto L, Duan H, Laudicella R, et al. Physiological 68Ga-RM2 uptake in patients with biochemically recurrent prostate cancer: an atlas of semi-quantitative measurements. Eur J Nucl Med Mol Imaging. 2020;47:115–22.
32. Barchetti F, Panebianco V. Multiparametric MRI for recurrent prostate cancer post radical prostatectomy and postradiation therapy. Biomed Res Int. 2014;2014:1–23.
33. Kitajima K, Hartman RP, Froemming AT, et al. Detection of local recurrence of prostate cancer after radical prostatectomy using endorectal coil MRI at 3 T: addition of DWI and dynamic contrast enhancement to T2-weighted MRI. Am J Roentgenol. 2015;205:807–16.
34. Kwon T, Kim JK, Lee C, et al. Discrimination of local recurrence after radical prostatectomy: value of diffusion-weighted magnetic resonance imaging. Prostate Int. 2018;6:12–7.
35. Vargas HA, Wassberg C, Akin O, Hricak H. MR Imaging of treated prostate cancer. Radiology. 2012;262:26–42.
36. Gaur S, Turkbey B. Prostate MR imaging for posttreatment evaluation and recurrence. Urol Clin N Am. 2018;45:467–79.
37. Haider MA, Chung P, Sweet J, et al. Dynamic contrast-enhanced magnetic resonance imaging for localization of recurrent prostate cancer after external beam radiotherapy. Int J Radiat Oncol. 2008;70:425–30.
38. Jager GJ, Barentsz JO, Oosterhof GO, Witjes JA, Ruijs SJ. Pelvic adenopathy in prostatic and urinary bladder carcinoma: MR imaging with a three-dimensional TI-weighted magnetization-prepared-rapid gradient-echo sequence. Am J Roentgenol. 1996;167:1503–7.
39. Thoeny HC, Froehlich JM, Triantafyllou M, et al. Metastases in normal-sized pelvic lymph nodes: detection with diffusion-weighted mr imaging. Radiology. 2014;273:125–35.
40. Padhani AR, Lecouvet FE, Tunariu N, et al. METastasis reporting and data system for prostate cancer: practical guidelines for acquisition, interpretation, and reporting of whole-body magnetic resonance imaging-based evaluations of multiorgan involvement in advanced prostate cancer. Eur Urol. 2017;71:81–92.
41. Clopper CJ, Pearson ES. The use of confidence or fiducial limits illustrated in the case of the binomial. Biometrika. 1934;26:404.
42. R Core Team (2019). R: a language and environment for statistical computing. R Foundation for Statistical Computing, Vienna. 2019. https://www.R-project.org/2019.
43. Minamimoto R, Hancock S, Schneider B, et al. Pilot comparison of 68 Ga-RM2 PET and 68 Ga-PSMA-11 PET in patients with biochemically recurrent prostate cancer. J Nucl Med. 2016;57:557–62.
44. Hoberück S, Michler E, Wunderlich G, et al. 68Ga-RM2 PET in PSMA- positive and -negative prostate cancer patients. Nuklearmedizin. 2019;58:352–62.